ELSEVIER

Fire Safety Journal **27** (1996) 265–287

Printed in Northern Ireland
0379-7112/96/$15·00

PII: S0379-7112(96)00056-2

Prediction of Fire Hazards Associated with Chemical Warehouses

S. D. Miles & G. Cox

Fire Research Station, Building Research Establishment, Garston, Watford, Hertfordshire WD2 7JR, UK

(Received 5 March 1996; revised version received 18 June 1996; accepted 5 July 1996)

ABSTRACT

This paper describes the application of computational fluid dynamics (CFD) to the task of predicting fire product emissions from warehouses containing hazardous materials. A growing pool fire is modelled inside a warehouse with automatic, heat-detector-operated roof vents and various prescribed external wind flows. The first 5 min of the fire are simulated, by which time the heat release rate of the fire has reached 26 MW and all vents have opened. It is found that the strong thermal and entrainment processes associated with the fire are such that moderate external winds have only a second-order influence on the mass, momentum and buoyancy fluxes of the emissions. The response time of the roof vents is found to have a significant effect on the transient behaviour of the emissions. The potential and limitations for using CFD models as part of a broader environmental hazard analysis are reviewed. Crown copyright © 1997 Published by Elsevier Science Ltd.

NOTATION

A	Area (m^2)
F_b	Vertical flux of buoyancy ($kg\,m\,s^{-3}$)
F_m	Vertical flux of momentum ($kg\,m\,s^{-2}$)
f	Fuel mixture fraction (–)
h	Enthalpy ($J\,kg^{-1}$)
k	Turbulence kinetic energy ($m^2\,s^{-2}$)
m	Mass (kg)
$\dot{m}$	Mass release rate ($kg\,s^{-1}$)
m_{fu}, m_{ox}	Fuel, oxygen mass fraction (–)

$\dot{Q}$ Heat release rate (MW)
R_{fu} Burning rate ($kg\,s^{-1}\,m^{-3}$)
RTI 'Response time index' ($m^{0.5}\,s^{0.5}$)
s Fuel:oxygen stoichiometric ratio (–)
T Temperature (°C)
t Time (s)
u Velocity ($m\,s^{-1}$)
$\dot{V}$ Volume flow rate ($m^3\,s^{-1}$)

Greek symbols
ΔH_c Heat of combustion ($J\,kg^{-1}$)
ϵ Dissipation rate of turbulence kinetic energy ($m^2\,s^{-3}$)
η Combustion efficiency (–)
ρ Density ($kg\,m^{-3}$)

1 INTRODUCTION

In 1982 the Commission of the European Communities (CEC) issued Directive 82/501/EEC on 'Major accident hazards of certain industrial activities'.[1] Often known colloquially as the Seveso Directive, after the 1976 accident, it was designed to prevent major accidents arising from industrial activities, and to limit the consequences to man and the environment of any such accidents that do occur. Later amendments to this Directive extended its scope to include, amongst other things, greater control of the storage of hazardous substances.

One consequence of the Directive, and its amendments, has been a recognition of the need to develop a robust methology for conducting major accident hazard analysis for individual sites. These include warehouses storing hazardous substances such as pesticides or herbicides. Fires in such buildings, and the resultant danger to people and the environment, are of particular concern. Incidents such as those at Basle in Switzerland[2] and Nantes in France[3] have highlighted these dangers. Such fires can pose a serious threat to people and the environment, with hazardous fire products transmitted through the air or into the local hydrological system.

Although relatively simplistic tools[4] are currently available to assist in the evaluation of warehouse fire hazards, these cannot deal with difficult aspects such as complex terrain, multiple roof vents or sprinkler systems. The two-layer zonal modelling method developed originally by Thomas *et al.*[5] and subsequently incorporated within computer codes by, for example, Mitler and Emmons[6,7] has been applied to this particular problem by, for example, Pagella and De Faveri.[8] Here, the temperature and

volumetric flow rate of smoke leaving through a fixed roof vent area are calculated for a prescribed fire source and air inlet (doorway) area. These may then be used in simple plume rise formulae to calculate external downstream concentrations (see for example Carter[9]).

The techniques of computational fluid dynamics (CFD), however, provide a more rigorous and general approach. By solving the conservation equations of physics at very many grid-node locations, the CFD model generates a detailed picture of the fluid flow and heat transfer processes. CFD has been used by various authors to model both fire development within enclosures such as buildings and external dispersion. It allows for arbitrary building arrangements, urban environments and natural topology. Recently it has been applied to the study of wind flows over forested hills.[10]

This paper describes the development and application of a CFD model for the purpose of hazard assessment associated with warehouse fires. The JASMINE[11] model is used to predict, in fine detail, the transport of heat, air and combustion products for a series of enclosure fire scenarios. Attention is focused on conditions inside the building and at vent and doorway openings. The model has been coupled to a separate CFD model of the atmospheric boundary layer[12] in order to compute downstream concentrations of combustion products. Details of this are described elsewhere.[13]

The study focuses on pesticides and herbicides, which are often stored as a suspension in a liquid such as xylene. The storage containers are generally stacked in a high-rack arrangement, which provides the potential for rapid vertical fire spread, and should flames reach the underside of the roof, there is the possibility of lateral spread to adjacent racks as a result of heat transfer from hot gases trapped beneath the roof. Lateral spread across the warehouse may also occur due to the spillage of flammable solvents from burst containers.

Warehouse fires have the potential to pollute the local environment in two ways. Once it has reached a certain size, a warehouse fire will generally result in the release of products of combustion from openings in the building structure into the surrounding atmosphere. Additionally, water runoff from fire fighting operations can cause condensed-phase combustion products and unburnt material to penetrate the local hydrological system.[14] This paper addresses only the airborne hazard.

The characteristics of an airborne release of toxic materials will vary from relatively small mass flow rates of low-buoyancy gases, leaking through adventitious ventilation openings, to much larger releases of highly buoyant gases through automatic roof vents, burnt-out skylights or eventually the collapsed roof. The buoyancy and momentum of the release will

be determined by the fire source, the building geometry, the ventilation and entrainment processes and the external wind pattern. The interaction of the buoyant plume(s) with the external air flow in the vicinity of the warehouse, and with adjacent buildings, will then determine the dispersion pattern of toxic material in the local environment.

In this paper, attention is restricted to the initial development of fire inside the building and subsequent emission of fire products into the external environment, with attention focused on the first 5 min from ignition. By this time any mitigation measures, such as sprinklers and/or roof vents, are likely to have operated. If the fire control measures fail, then the fire is likely to spread throughout the building. In this eventuality the roof may collapse and allow the entire warehouse contents to burn. This scenario, though of importance, is not addressed here.

2 THE PROBLEM STUDIED

A specific warehouse geometry was selected for numerical convenience, which is reasonably representative of many modern buildings of European design. The building, shown in Fig. 1, is 70 m long, 30 m wide and 8 m high and has a flat roof. Two doorway openings are located in one of the long walls. An array of 16 roof vents is also included; each vent is shown in the figure with an identification number used in the results section. The warehouse is located on flat terrain, and there is a prescribed wind flow from one direction, normal to the longer side, such that both doorways are either upstream or downstream.

The authors have previously reported results from modelling the internal fire development, and associated external dispersion, for a high-rack fire inside a warehouse with two doors and nine open roof vents.[13] In that work, the vent emissions were used as source terms for an atmospheric dispersion model. The fire source, derived from an experiment with a single high-rack of solid material,[15] had a heat release rate reaching 8.5 MW after 3 min. The dispersion model showed that with a $10\,m\,s^{-1}$ free-stream wind the external emission 'lifted off' significantly from the ground a short distance from the building.

This paper studies in more depth the fire development within the warehouse and the vented emissions of combustion products and entrained air. The effect of different wind patterns on the vent emissions is investigated. Each roof vent is closed initially, and subsequently opened during the course of a transient simulation according to the temperature rise of an associated 'fusible-link' heat detector. The fire source selected for this study is a growing pool fire of xylene, derived from experimental

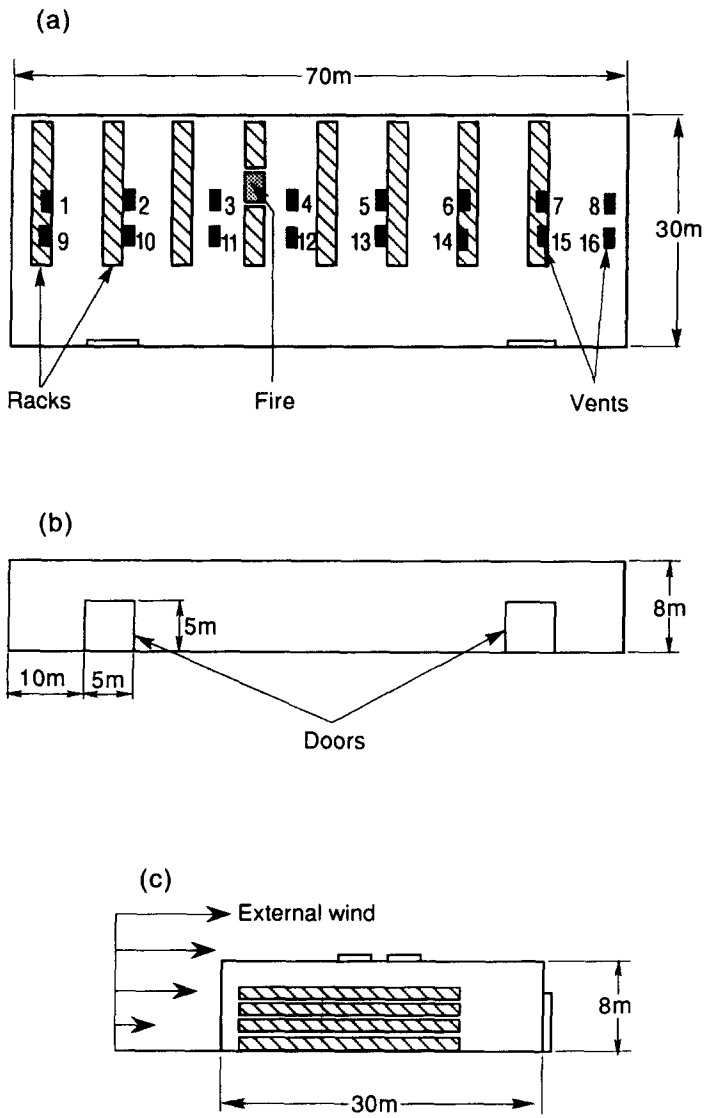

Fig. 1. Warehouse geometry. (a) Top view. (b) End view. (c) Side view.

data[16] for a burning pallet load of the solvent, and reaching 26 MW in 3 min.

An external wind may have a significant effect on the air flow inside the building and hence also the emission from the openings. Two external wind conditions are investigated, with free-stream wind speeds of $5\,m\,s^{-1}$ and $10\,m\,s^{-1}$ respectively. Over the flat terrain chosen, wind speed

increases with height from zero at ground level to the free-stream value at the top of the atmospheric boundary layer.

Each of the 16 roof vents is operated by a heat detector located just below. Each vent has dimensions 1.25 m by 2.5 m, giving a total vent area of 50 m^2, equal to the total area of the two doorways (each 5 m by 5 m). Allowing individual roof vents, or groups of vents, to open at different times makes the simulations more realistic. The effect of detector response is examined. An arrangement of storage racks is also included, and the pool fire is located in a gap in the racks. The location of the doorways and racks may influence the entrainment process.

Xylene is a typical solvent used to store organophosphorus and other pesticide products. A high-rack containing bottles of such products will tend to burn such that the solvent escapes from ruptured containers into a growing spillage fire below. The main characteristics of both the internal flow and the emissions may be captured by modelling the fire source as a pool of solvent alone. It is the buoyancy and momentum of the emissions through individual vents that determine how they are dispersed within the local environment.

Assuming that the composition of the combustion products is known, and that they do not continue to react beyond the flame tip, the dispersion pattern of a particular sub-species may be derived from the dispersion of the complete emission. The 'active' material will itself either burn, generating a range of toxic and non-toxic products, or survive and be transported in the thermal plume unaffected. To predict the dispersed concentration of, for example, surviving active material therefore requires some form of empirical data for the survival fraction at the fire source. Careful experimental procedures are required to obtain yields of toxic products and active material survival fractions (see, for example, Smith-Hansen and Jørgensen[17] and Atkinson and Jagger[18]).

Atkinson[16] reports an experiment involving the burning of a pallet-load of bottles containing xylene, in which the mass loss of the pallet was measured with time. These data have been used in the current study to define the growing pool fire, where it has been assumed that the drainage rate of xylene from the pallet matches its mass burning rate. This assumption is appropriate if the spilled solvent spreads out across the warehouse floor without constraint, representing a 'worst case' scenario. Bunding, or other control measures, would reduce the spreading of the pool and hence the peak heat release rate of the fire. Conversely, if more pallet-loads were involved in the initial fire, then the fire might be more severe than that modelled.

The method for computing the area and burning rate of the xylene pool

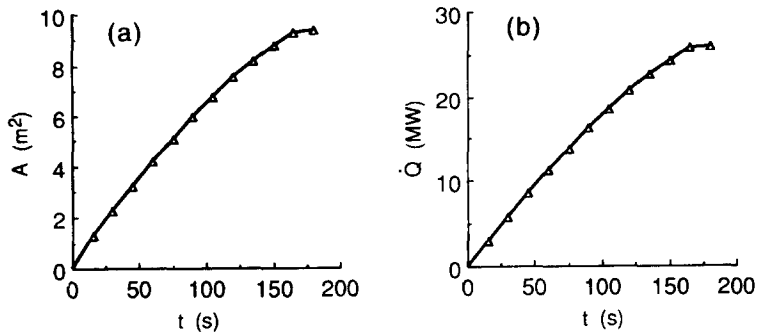

Fig. 2. Growing pool fire. (a) Area. (b) Heat release rate.

fire, at each time step, is described in the next section. Figure 2 shows the resulting pool area and heat release rate as functions of time. The combustion model used calculates concentrations of the primary products of combustion, namely water and carbon dioxide. No attempt has been made to predict other products of combustion or the concentration of 'surviving' active material, but the dispersion of active material may be deduced from the calculation of mixture fraction, f.

3 DETAILS OF THE MODELLING

JASMINE has been developed to allow predictions of internal warehouse fire development, the resultant emissions of fire products from multiple roof vents and the influence of prescribed wind patterns. Although no comparisons have been possible with full-scale warehouse data, JASMINE has previously been validated for a wide range of scenarios.[11,19–21]

The main elements of the solution method have been described elsewhere.[22] Summarising, the SIMPLEST pressure-correction method[23] is employed on a structured Cartesian grid. A staggered velocity arrangement is used, and discretization of the convection terms is by the first-order upwind scheme. For transient simulations the solution is advanced by a first-order, fully implicit scheme.

The two-equation k,ϵ model is employed to incorporate the effects of turbulent mixing, with buoyancy source terms included in both the momentum and turbulence equations.[24] A six-flux radiation model[25] was used with the absorption coefficient of combustion products set at $0.3\ m^{-1}$.

Other features of the model of specific relevance to the warehouse problem are described below.

3.1 Combustion chemistry

An important feature of fires is that the mean rate of chemical reaction is influenced strongly by the local turbulent mixing process. The hydrodynamic mixing of air and fuel is much slower than the rate of chemical reaction, and it is this physical mixing which controls the local rate of fuel disappearance.

JASMINE employs an eddy dissipation model[26] to incorporate combustion and mixing. The rate of fuel consumption, R_{fu}, is assumed to be

$$R_{fu} = C_R \rho \frac{\varepsilon}{k} \min\left(m_{fu}, \frac{m_{ox}}{s}\right) \tag{1}$$

where C_R is a constant, m_{fu} and m_{ox} are the mass fractions of fuel and oxygen respectively and s is the fuel:oxygen stoichiometric ratio. Equation (1) implies that in air-rich locations the rate of reaction is controlled by the availability of fuel and in fuel-rich locations by the availability of air.

The eddy dissipation model is incorporated by solving scalar transport equations for m_{fu} (R_{fu} as the source term) and the mean normalised mixture fraction, f, defined as

$$f = \frac{\left(m_{fu} - \frac{m_{ox}}{s}\right) + \frac{m_{ox,0}}{s}}{m_{fu,1} + \frac{m_{ox,0}}{s}} \tag{2}$$

where the subscripts 0 and 1 denote conditions in ambient air and the fuel supply respectively.

Combining the above model with a simple one-step chemical reaction allows the concentration of the stable species carbon dioxide and water vapour to be predicted throughout the domain. For xylene the assumed one-step reaction was

$$2C_8H_{10} + 21O_2 \rightarrow 10H_2O + 16CO_2 \tag{3}$$

This is sufficient to enable the physical parameters of the vented emissions to be computed. However, if the concentration of other chemical species is required, e.g. carbon monoxide, hydrogen cyanide and unburnt active material, then experimental correlations or a more elaborate combustion model are needed, for example the laminar flamelet model.[27] Although applied to simpler fire problems,[28] this model has not been adopted here.

3.2 Boundary conditions

Open boundaries were imposed at a distance 15 m from the building walls and roof, except upstream, where an inflow velocity profile was prescribed 10 m away. Open boundaries may be imposed in a variety of ways. However, for the purpose of modelling the internal fire development, and the subsequent venting of combustion products, it was considered sufficient to use fixed-pressure boundary conditions, i.e. pressure and normal gradients at these boundaries set to zero.[24]

Inflow velocity data at the upstream boundary had been computed previously by a CFD model of the external environment. Detailed data were available for both 5 and 10 m s^{-1} free-stream wind conditions. The presence of the warehouse in this boundary layer had been included, causing a perturbation to the simple boundary layer profile. It was necessary to interpolate these data to fit the JASMINE grid.

No-slip boundary conditions were applied on the inside and outside of the warehouse and at the ground. Standard wall functions were used for computing momentum losses and near-wall k,ϵ turbulence values. The effect of ground roughness due to trees, other buildings etc. was not included. Other boundary conditions and source terms are now described.

3.2.1 *Heat transfer to solid surfaces*

Heat transfer to solid surfaces is important for a number of reasons, including:

- heat removed from the gas phase may have an important effect on the fluid dynamics;
- to predict the thermal response and possible structural failure of the building; for a warehouse this may include the heating and subsequent collapse of plastic skylights.

Convection and radiation fluxes to the solid surfaces were calculated and included as sink terms in the enthalpy equation. If it is then assumed that these fluxes are balanced by a one-dimensional conduction flux into the solid, and that the solid can be approximated as a semi-infinite boundary, the surface temperatures may be calculated.[22]

3.2.2 *Fire source*

The coupling of the gas-phase transport processes with the burning characteristics of a solid or liquid fuel is the cause of many difficulties in the mathematical modelling of fires. The solid and liquid commodities and packaging materials encountered in chemical warehouses are, in general, non-homogeneous. A stored item may comprise a combination of

cardboard, plastic, flammable solvent, granular agrochemical, wood and metal. Such materials are not readily amenable to rigorous theoretical analysis. For this reason, large-scale calorimetry or another experimental approach is essential for the provision of input data to fire models.

A growing pool fire of xylene provided the fire source for the results presented in this paper. More specifically, the pool area, fuel mass release rate and heat release rate were calculated at each time step, assuming that the area of the pool was such that the total burning (fuel mass loss) rate equalled the drainage rate of xylene from the ruptured bottles above. The drainage rate information was derived from experimental data.[15]

The following strategy was adopted for determining the transient fire source:

- The following equation was fitted, approximately, to the experimental data for the (declining) mass of the pallet load m_p:

$$m_p(t) = -\alpha e^{-\beta t^2} \tag{4}$$

- Equation (4) was differentiated to give an expression for the drainage rate of xylene from the pallet:

$$\dot{m}_p(t) = 2\alpha\beta t e^{-\beta t^2} \tag{5}$$

- Equation (5) was then equated with an empirical formula for the burning rate of xylene pool fires $\dot{m}_f$:[29]

$$\dot{m}_f = 0.09A(1 - e^{-2.8(\frac{A}{\pi})^{1/2}}) \tag{6}$$

- The non-linear eqn (6) was solved iteratively to yield the pool area A.
- An appropriate number of grid nodes were allocated, at time t, so that the total area of the fire source, A_f, in the JASMINE simulation was as close as possible to A.
- The heat release rate $\dot{Q}_f$ was then defined as

$$\dot{Q}_f(t) = \dot{m}_f(t)\Delta H_c \eta \tag{7}$$

where ΔH_c is the heat of combustion of the fuel, taken as 4.13×10^7 J kg^{-1}, and η is the combustion efficiency, taken as 0.75 in the current simulations.

Ninety-six grid cell faces in a 12 by 8 array, each cell representing a floor area of 0.0977 m^2, were 'reserved' for the fire source. Starting with just a few cells, more were added as the simulation progressed, giving the total fire area and heat release rate shown in Fig. 2. In the simulations the fire area was truncated to 9.38 m^2 after 167 s, at which time all 96 cells

were allocated and the heat release rate had reached 25.9 MW. The fire was then assumed to be steady at this heat release rate and floor area.

3.3 Roof vent operation

Each roof vent was assumed to open when a single fixed-temperature (fusible-link) heat detector, located 0.125 m below the vent, reached a critical temperature T_{op}. Detector temperature rise was determined from the following equation (see, for example, Schfiliti[30]), which accounts only for convective heat transfer from the surrounding gas to the detector:

$$\frac{d}{dt}\left(T_d\right) = |\underline{u}_d|^{1/2}\left(\frac{T_g - T_d}{\mathrm{RTI}}\right) \tag{8}$$

where T_d and T_g are the temperatures of the detector and surrounding gas respectively, $|\underline{u}_d|$ is the magnitude of the gas velocity at the detector, and RTI is the *response time index* of the detector. The effects of thermal radiation on detector operation have been ignored in this study but could be incorporated in future studies.

Equation (8) has been incorporated into JASMINE by the following finite-difference formula:

$$T_d^{[i]} = \frac{1}{(1-\beta^{[i]})}[(1-\beta^{[i]})T_d^{[i-1]} + \beta^{[i]}(T_g^{[i-1]} + T_g^{[i]})] \tag{9}$$

where

$$\beta^{[i]} = \frac{1}{2.83\,\mathrm{RTI}}(t^{[i]} - t^{[i-1]})(\,|\underline{u}_d|^{[i]} + \,|\underline{u}_d|^{[i-1]})^{1/2} \tag{10}$$

and $[i]$ and $[i-1]$ denote the *current* and *previous* time steps respectively.

Two combinations of RTI and T_{op} were used in this study.

3.4 Solution procedure and grid specification

For each scenario a steady-state simulation was first performed at ambient temperature with all vents closed, both doorways open, and no fire. This established the influence of the external wind on the internal air flow. A transient simulation was then performed with the growing fire and staggered vent operation. A fixed time step of 1 s was used, except for the first 5 s, for which the time step was 0.5 s. A limited sensitivity analysis was performed with the time step reduced by half.

The same grid was used for the various scenarios reported. A total of 88 608 cells were used, with 48, 71 and 26 cells in the width, length and vertical directions respectively (see Fig. 1). Of these, 45 360 were inside

TABLE 1
Scenarios Modelled

Scenario	*Free-stream wind speed* ($m\,s^{-1}$)	*Doorway location*	*Roof vent (detector) response*
1	5	downstream	I
2	5	downstream	II
3	10	downstream	II
4	5	upstream	II
5	zero	n/a	II

the warehouse itself. Vents 1 to 8 were each represented by an array of 12 cells, whilst vents 9 to 16 were represented by only four. A limited grid refinement analysis was performed with a 96 by 142 by 52 grid (708 864 cells).

4 SELECTED SCENARIOS AND RESULTS

Table 1 summarises the scenarios modelled. Roof vent response here refers to the behaviour of the heat detector located below each vent. Table 2 presents the RTI and operating temperature for the I (faster) and II (slower) classifications. These do not correspond to any industry standard. Ambient temperature was 17°C for all scenarios.

RTI values of 50 and 200 $m^{0.5}\,s^{0.5}$ correspond respectively to a 'fast response' device and a more typical device. The fastest commercial fusible links have an RTI of ~22 $m^{0.5}\,s^{0.5}$ (designed primarily for residential systems), while 'standard' links can have values up to ~400 $m^{0.5}\,s^{0.5}$. The two operating temperatures in Table 2 correspond to 40°C and 60°C rise above ambient.

Substantial data were generated for each scenario. In particular, detailed transient data were recorded for the inflow and/or outflow at

TABLE 2
RTI and Operating Temperature of the Heat Detectors

Classification	*RTI* ($m^{0.5}s^{0.5}$)	*Operating temperature* (°C)
I	50	57
II	200	77

each opening. These data included mass and heat flow rates, velocities, temperatures, species mass fractions, densities and other solved scalars such as turbulent kinetic energy.

At each roof vent the vertical fluxes of buoyancy force (F_b) and momentum (F_m) were calculated. These are defined as

$$F_b = \dot{V}_e(\rho_a - \rho_e)g \tag{11}$$

$$F_m = \dot{V}_e \rho_e w_z \tag{12}$$

where $\dot{V}_e$ is the volumetric flow rate of the emission, ρ_a and ρ_e are ambient and emission density respectively, g is the acceleration due to gravity and w_z is the vertical velocity component of the emission.

These quantities are related as follows to the fluxes of buoyancy (F) and momentum (M) used commonly in plume rise calculations:[31]

$$F = \frac{F_b}{\rho_a \pi} \tag{13}$$

$$M = \frac{F_m}{\rho_a \pi} \tag{14}$$

When considering emissions from chimneys, the buoyancy 'flux' F is sometimes referred to as the 'stack parameter'.[32] In this study, attention has been restricted to the quantities F_b and F_m in eqns (11) and (12). The relative magnitude of these two quantities provides a measure of the relative importance of buoyancy and momentum in the emission.

For all scenarios studied it was found that at ~4–5 min from the start of the fire, conditions are approaching steady-state. All roof vents have activated by this time. The heat from the fire is either convected through the vents or transferred to the warehouse structure and the commodity storage arrays. In addition to combustion products, entrained air and unburnt fuel are also emitted through the vents. In these well-ventilated examples virtually all the entrained air enters through the two doorways, and the amount of unburnt fuel leaving through the roof vents is insignificant.

As an example, Table 3 shows the values of various key parameters, at each vent, for scenario 1 after 5 min. The vent numbering is as shown in Fig. 1. The mass flux includes combustion products and entrained air; m_{pr} indicates the proportion that is combustion product. The mass and momentum fluxes have evened out across the vents by this stage. However, for other parameters, such as m_{pr} and F_b, there is a greater variation between vents located near the fire and those further away.

A secondary feature of the data is that the mass flux is greater through

TABLE 3
Roof Vent Emission Data for Scenario 1 after 5 min

Vent no.	*Mass flux* ($kg\,s^{-1}$)	m_{pr} (–)	*Convected heat flux* (*MW*)	F_m ($kg\,m\,s^{-2}$)	F_b ($kg\,m\,s^{-3}$)	*Temp.* (°C)
1	7.05	3.89×10^{-2}	1.64	24.3	50.6	229
2	7.30	3.48×10^{-2}	1.71	25.3	53.6	235
3	6.05	5.76×10^{-2}	2.13	21.9	66.1	356
4	5.94	5.74×10^{-2}	2.19	22.4	66.9	360
5	7.78	3.44×10^{-2}	1.76	28.0	54.7	225
6	8.01	2.77×10^{-2}	1.26	25.4	39.3	161
7	7.32	2.46×10^{-2}	1.02	20.9	32.3	145
8	7.15	2.34×10^{-2}	1.09	21.4	34.2	157
9	7.43	3.24×10^{-2}	1.47	23.5	45.2	195
10	7.52	2.28×10^{-2}	1.29	22.7	39.9	173
11	7.26	2.38×10^{-2}	1.30	21.7	40.3	180
12	7.49	3.04×10^{-2}	1.60	24.8	49.4	211
13	7.83	2.91×10^{-2}	1.40	25.0	43.4	179
14	7.92	2.78×10^{-2}	1.08	23.4	33.8	141
15	7.26	2.23×10^{-2}	0.83	18.9	26.2	121
16	7.36	2.03×10^{-2}	0.96	21.1	30.0	135
TOTAL	116.7	3.16×10^{-2}	22.72	369.5	688.8	200

the vents on the downwind side of the roof, i.e. numbers 9 to 16 (this difference was highlighted further in the grid refinement study, discussed in the next section).

A final steady-state simulation was performed for scenario 1 with the fire source fixed at its maximum output of 25.9 MW. A 'steady-state time' of 30 min was assumed in calculating heat losses to the building and storage arrays. Emission parameters do not change significantly from those after 5 min. The only difference of any note is in the heat loss to the building and storage arrays, which is 10% after 5 min and 7% at 'steady-state'.

The initial flow pattern inside the warehouse before the fire varies with the wind configuration. After 4 min however, the vent emissions and doorway air flows are similar for each scenario. By the time conditions have reached steady values, the influence of the fire is significantly greater than that of the external wind flows modelled. Table 4 summarises the initial (inflow) conditions and the main emission data, after 4 min, for each of the five scenarios. For all scenarios the first vent to open is number 4, followed by number 3. These are the two closest to the fire source (see Fig. 1).

TABLE 4
Summary Information for All Scenarios

Scenario	*Pre-fire air flow through building* ($kg\,s^{-1}$)	*Total emission from vents after 4 min*				*Vent opening time (s)*	
		Mass flux ($kg\,s^{-1}$)	*Convected heat flux* (MW)	F_m ($kg\,m\,s^{-2}$)	F_b ($kg\,m\,s^{-3}$)	*First*	*Last*
1	2.0	116	22.4	362	678	21	120
2	2.0	116	23.3	376	693	45	211
3	3.2	122	24.1	414	720	45	213
4	7.6	134	24.2	502	708	45	223
5	0.0	107	25.6	324	666	45	208

After 4 min the total emission of combustion products from the warehouse is similar for all five scenarios, as are the convected heat and buoyancy fluxes. However, comparing scenarios 2, 3 and 5, it is seen that with the doorways downstream the effect of increasing the external wind speed is to produce a higher momentum flux and a slightly higher mass flux at the vents. A greater effect is produced by placing the doorways upstream (compare scenarios 2 and 4), which again increases the mass and momentum fluxes at the vents.

The 'slower' (II) detectors take about twice as long to operate as the 'faster' (I) ones. This clearly has an important bearing on the quantity of toxic material that may be emitted in the early stages of a fire. It draws attention to the debate on whether to provide fire vents in hazardous storage warehouses, and to the complex trade-off between atmospheric emission and the ability to control fire development and provide safety inside the building.

Table 5 provides further information on the emissions after 4 min. The scalar values here are area averages over all 16 vents, while the average velocity is the value that would apply if mass flow rate and density were uniform across the vents.

Considering now the transient behaviour in more detail, Fig. 3 shows the emission of combustion products during the first 4 min, at a selection of individual vents, for scenarios 1 and 2. For both scenarios it is observed that after each vent opens it takes ~90 s for the emission from that vent to settle to a 'steady' value. Furthermore, the earlier a vent opens, the greater the final (steady) emission of combustion products. The most significant difference between the two scenarios is that for the 'slower' vents the initial emission of combustion products at each vent, just after it opens, is about twice that for the 'faster' vents. This is caused by a greater

TABLE 5
Emission Data after 4 min

Scenario	*Average scalar value at vents*			*Outflow velocity* ($m\ s^{-1}$)	
	m_{pr}	m_{fu}	*Temperature* (°C)	*Average*	*Maximum*
1	3.2×10^{-2}	2.2×10^{-6}	198	1.9	4.5
2	3.3×10^{-2}	0.9×10^{-6}	204	1.9	4.6
3	3.2×10^{-2}	1.3×10^{-6}	203	2.0	5.2
4	2.9×10^{-2}	1.6×10^{-6}	185	32.2	5.7
5	3.5×10^{-2}	1.7×10^{-6}	213	1.8	4.2

buoyancy head in the smoke layer before the opening of the vent. There is a tendency for emissions from an individual vent to 'overshoot' before settling to their steady state. This is less pronounced, or absent altogether, for the 'faster' vents.

Figure 4 shows a selection of m_{pr} contours for scenario 1 after 4 min. Two orthogonal planes are shown, one through the fire source and the 'upstream' row of vents, and the other through vents 4 and 12. It is observed that the presence of the roof vents and open doorways keeps conditions inside the warehouse reasonably safe at head height and below. Figure 5 shows the product mass fraction contour of 5×10^{-3} for scenario 1 after 4 min. To set these m_{pr} values in perspective, a value of 1.4×10^{-3} would correspond approximately to a 20 m visibility through the smoke generated by a free-burning polyurethane foam mattress.[33]

5 GRID AND TIME STEP REFINEMENT

The results presented above were generated with a grid which, although using nearly 90 000 nodes, is still relatively coarse. To investigate the sensitivity of the solution to the grid, the final steady-state simulation for scenario 1 was repeated with a 'double-resolution' grid using twice as many nodes in each coordinate direction. This yielded just over 700 000 grid cells, which, although tolerable for a limited analysis, was too large for routine study on the hardware available.

Table 6 summarises some of the roof vent emission data for the final steady-state simulation for scenario 1 with the 'original' and 'double-resolution' grids. The finer grid produces a small influx of entrained air through vents 1 to 8 (upwind side), absent with the original grid.

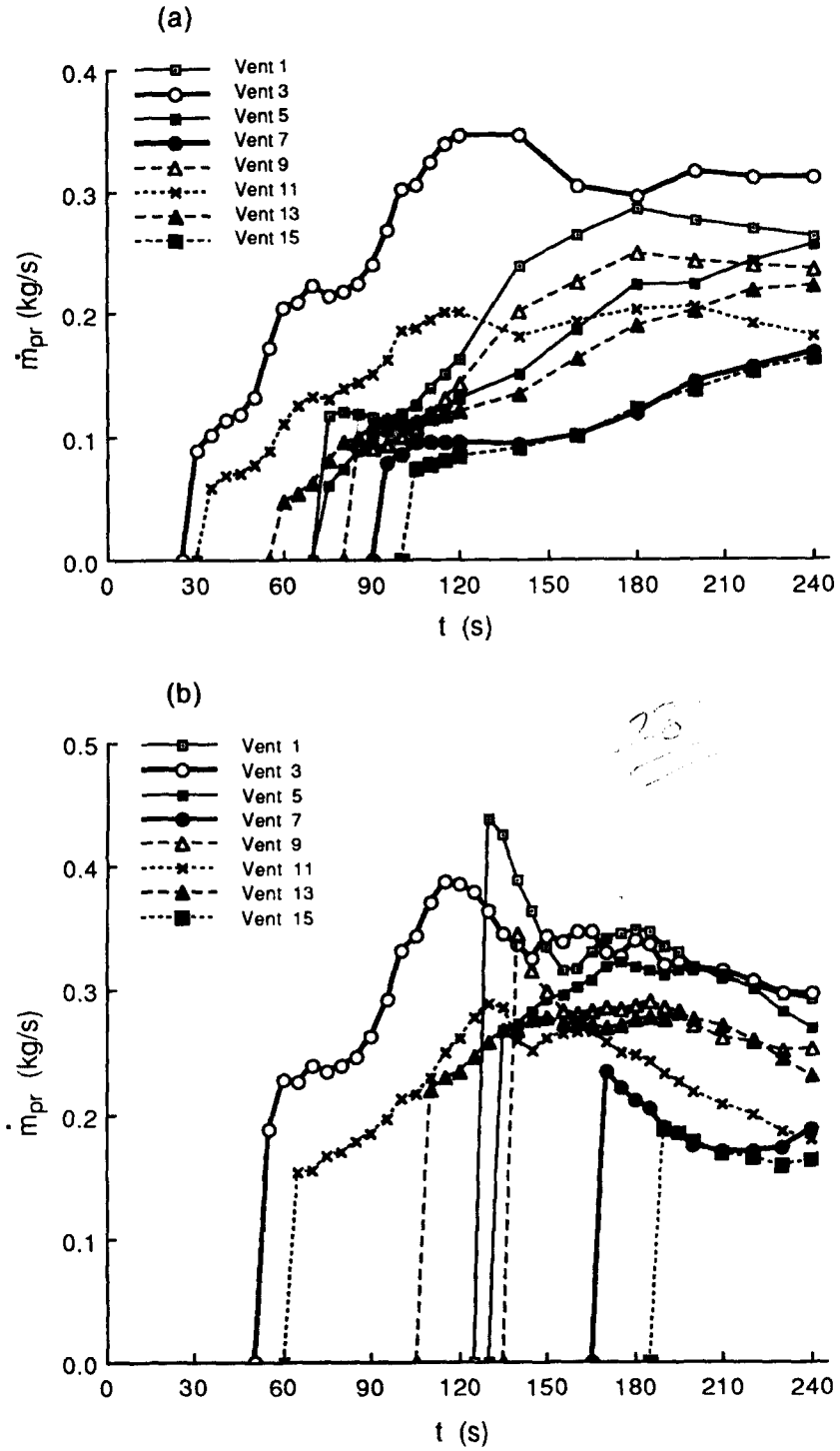

Fig. 3. Emission of combustion products from selected vents. (a) Scenario 1 ('fast' vents) (b) Scenario 2 ('slow' vents).

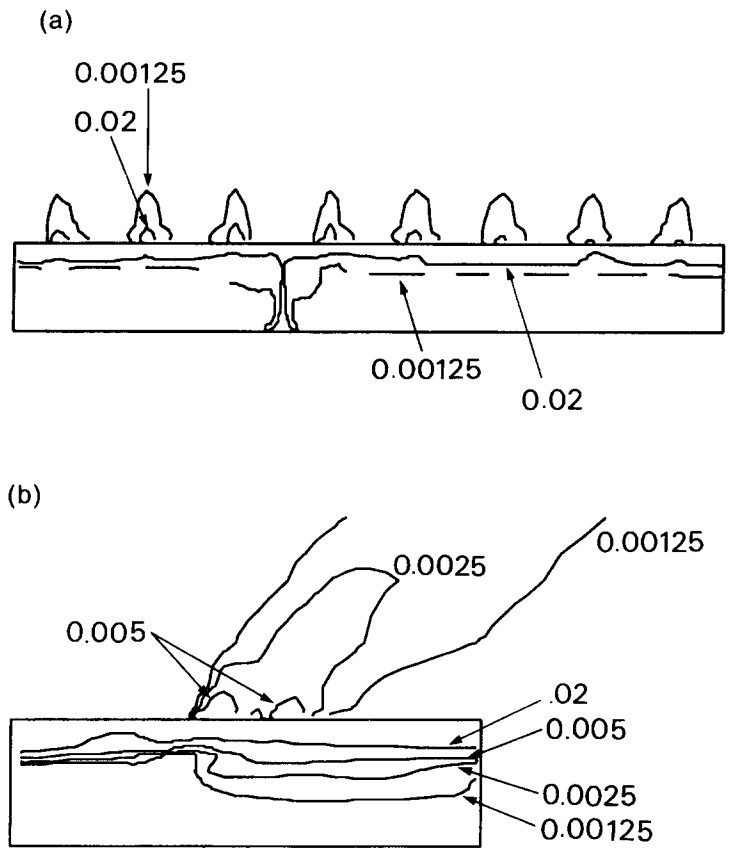

Fig. 4. Contours of m_{pr} for scenario 1 after 240 s. (a) End view in plane through fire (showing presence of racks). (b) Side view in plane through vents 4 and 12.

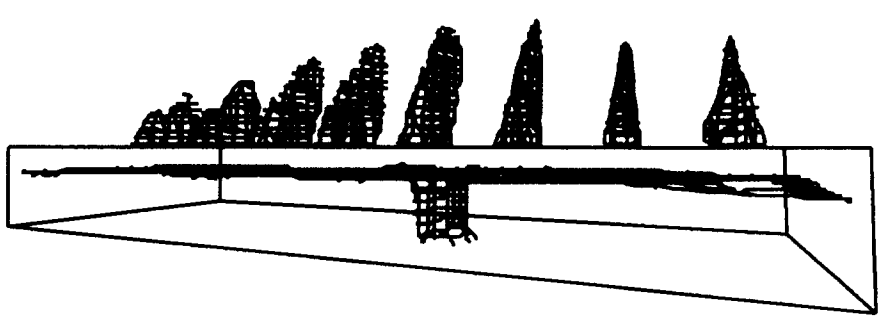

Fig. 5. Contour of m_{pr} 0·005 for scenario 1 after 240 s (viewed from upstream).

TABLE 6
Grid Refinement for Scenario 1

Grid	*Final steady values at vents*						
	m_{fr} (–)	*Mass flux out* ($kg\,s^{-1}$)	*Mass flux in* ($kg\,s^{-1}$)	*Convected heat flux* (MW)	F_m ($kg\,m\,s^{-2}$)	F_b ($kg\,m\,s^{-3}$)	*Average temp.* (°C)
Original	3.1×10^{-2}	117.9	~0	24.1	392	724	209
Double-resolution	2.7×10^{-2}	129.7	0.34	24.1	467	721	186

Approximately half of this 'new' inflow is through vent 4. The total mass and momentum fluxes are slightly higher with the finer grid. These differences indicate that the solutions presented in the paper are not completely grid-independent. In the finer grid there are 48 cells in vents 1 to 8 and 16 in vents 9 to 16 (compared with 12 and 4 respectively in the original grid).

An aspect of CFD applications that is often overlooked is the sensitivity to the time step used in transient simulations. JASMINE, in common with many codes, uses a first-order, fully implicit temporal discretization, which although numerically stable is still susceptible to temporal error if the time step is too great. The results presented above used a fixed time step of 1 s (except for the first 5 s). To investigate the sensitivity to the time step, the first 120 s of scenario 1, using the original grid, were repeated with the time step reduced by half.

It was found that there was no significant difference in the results obtained with the reduced time step. To illustrate this, Table 7 presents various data obtained with the two time steps.

6 DISCUSSION AND CONCLUSIONS

This work represents an important step in the development of a CFD capability for estimating the emissions of fire products from buildings. Time-dependent mass, momentum and buoyancy fluxes can be generated at multiple openings in the building. Such data, together with toxic-concentration information, may be used as source terms for environmental dispersion models. This allows prediction of the potential hazard to the

TABLE 7
Time Step Refinement for Scenario 1

Time step (*s*)	*Time for vents to open* (*s*)			*Total emission from vents after* 120 *s*			
	First	*Second*	*Last*	*Mass flux* ($kg\,s^{-1}$)	*Convected heat flux* (*MW*)	F_m ($kg\,m\,s^{-2}$)	F_b ($kg\,m\,s^{-3}$)
1.0	21	24	120	98.6	15.2	258	444
0.5	21	23.5	120	98.0	15.0	255	441

environment and local population from warehouse fires, and could form part of a more general hazard assessment.

A CFD model allows a more detailed description of the dispersion source terms than is possible with more traditional zonal-type models. Furthermore, the model allows roof vents to open during the course of a simulation, and includes the effect of an external wind pattern on conditions inside the building.

The first 5 min of a spillage pool fire in a representative warehouse have been modelled. Over this period a sequence of roof vents were opened according to the temperature rise of associated fusible-link heat detectors. Comparison simulations have been performed with various external wind conditions and with different response heat detectors. For free-stream wind speeds up to $10\,m\,s^{-1}$ it was found that the buoyancy and entrainment processes associated with the fire itself determined the main characteristics of the emissions from the vents. Wind speed and direction had only a secondary influence.

Further work is needed to address cases where the wind is 'oblique' to the building and where doors are shut with only adventitious leakage providing opportunities for emissions. As always with CFD, finer-grid solutions are required to ensure truly grid-converged results. It would also be preferable to exploit curvilinear coordinates for dealing with sloped roofs and oblique wind patterns.

In the project described here, a CFD model has been used to generate emission data which can be used subsequently in a separate dispersion model to predict the flow of combustion products in the local environment. CFD provides one option for the external dispersion model. Christolis *et al.*[34] have studied in depth the modelling of the dispersion of warehouse fire combustion products using this approach. However, when using CFD for both the internal (fire) and external (dispersion) regimes,

it would be desirable to use just one model, thus permitting more direct interaction. This would necessitate the use of multi-block or fully unstructured grids.

ACKNOWLEDGEMENTS

This work was performed under the Science and Technology for Environmental Protection (STEP) programme of the Commission of the European Communities (CEC), and was funded jointly by the CEC and the BRE Chief Executive's Strategic Research Programme.

REFERENCES

1. Council directive of 24 June 1982 on the major-accident hazards of certain industrial activities (82/501/EEC), *Off. J. Eur. Commun.* (L230) (1982) 1.
2. Sandoz—an ecological disaster, *Fire Int.* **102** (Dec.–Jan.) (1986–87) 17.
3. Fertilizer warehouse, Nantes, France, *Fire Prev.*, **209** (1988) 50.
4. Atkinson, G., Notes for the use of FIREPEST: a computer model of fire in a warehouse and the dispersion of toxic products of combustion. Unpublished document, Health and Safety Executive (UK), 1990.
5. Thomas, P. H., Hinkley, P. L., Theobald, C. R. & Simms, D. L., Investigations into the flow of hot gases in roof venting. Fire Research Technical Paper No. 7, HMSO, London, 1963.
6. Emmons, H. W., The prediction of fires in buildings. In *Seventeenth Symposium (International) on Combustion*. The Combustion Institute, Pittsburgh, PA, 1979, pp. 1101–11.
7. Mitler, H. E., Mathematical modeling of enclosure fires. In *Numerical Approaches to Combustion Modelling*, ed. E. S. Oran & J. P. Boris. American Institute of Aeronautics and Astronautics, Washington, DC, 1991, pp. 711–54.
8. Pagella, C. & De Faveri, D. M., Fire in industrial buildings: simulation of fire growth, smoke production and venting. *Trans. Inst. Chem. Eng. B*, **71** (1993) 180–186.
9. Carter, D. A., Dispersion of toxic combustion products from large fires. *Fire Technol.*, **28** (1992) 168–173.
10. Kobayashi, M. H., Pereira, J. C. F. & Siqueira, M. B. B., Numerical study of the turbulent flow over and in a model forest on a 2D hill. *J. Wind Eng. Industr. Aerodyn.*, **53** (1994) 357–374.
11. Cox, G. & Kumar, S., Field modelling of fire in forced ventilated enclosures. *Combust. Sci. Technol.*, **52** (1987) 7–23.
12. Markatos, N. C., Pericleous, K. & Simitovic, R., A hydrometeorological three-dimensional model of thermal energy releases into environmental media. *Int. J. Num. Meth. Fluids*, **7** (1987) 263–276.

13. Miles, S. D., Cox, G., Christolis, M. N., Christidou, C. A., Boudouvis, A. G. & Markatos, N. C., Modelling the environmental consequences of fires in warehouses. In *Fire Safety Science, Proceedings of the 4th International Symposium*. The International Association for Fire Safety Science, 1994, pp. 1221–32.
14. McQuaid, J., Industrial fire problems: an overview. In *Fire Safety Science, Proceedings of the 3rd International Symposium*. Elsevier Applied Science, 1991, pp. 61–81.
15. You, H. Z. & Kung, H. C., Strong buoyant plumes of growing rack storage fires. In *Twentieth Symposium (International) on Combustion*. The Combustion Institute, Pittsburgh, 1984, pp. 1547–54.
16. Atkinson, G. T., Fire spread in a pallet load of bottles of flammable liquid. *Fire Safety J.*, **22** (1994) 409–415.
17. Smith-Hansen, L. & Jørgensen, S. F., Combustion products from pesticides and other chemical substances determined by use of DIN 53 436. *Fire Safety J.*, **23** (1994) 51–66.
18. Atkinson, G. T. & Jagger, S. F., Assessment of hazards from warehouse fires involving toxic materials. *Fire Safety J.*, **22** (1994) 107–123.
19. Kumar, S., Gupta, A. K. & Cox, G., Effects of thermal radiation on the fluid dynamics of compartment fires. In *Fire Safety Science, Proceedings of the 3rd International Symposium*. Elsevier Applied Science, 1991, pp. 345–54.
20. Cox, G., Kumar, S. & Markatos, N. C., Some field model validation studies. In *Fire Safety Science, Proceedings of the 1st International Symposium*. Elsevier Applied Science, 1986, pp. 159–71.
21. Kumar, S., Field model simulations of vehicle fires in a Channel Tunnel shuttle wagon. In *Fire Safety Science, Proceedings of the 4th International Symposium*. The International Association for Fire Safety Science, 1994, pp. 995–1006.
22. Cox. G, Compartment fire modelling. In *Combustion Fundamentals of Fire*, ed. G. Cox. Academic Press, New York, 1995.
23. Spalding, D. B., Mathematical modelling of fluid mechanics, heat transfer and chemical reaction processes. CFDU Report HTS/80/1, Imperial College, London, 1980.
24. Markatos, N. C., Malin, M. R. & Cox, G., Mathematical modelling of buoyancy-induced smoke flow in enclosures. *Int. J. Heat Mass Transfer*, **25** (1982) 63–75.
25. Gosman, A. D. & Lockwood, F. C., Incorporation of a flux model for radiation into a finite-difference procedure for furnace calculations. In *Fourteenth Symposium (International) on Combustion*. The Combustion Institute, Pittsburgh, PA, 1973, pp. 661–73.
26. Magnussen, B. F. & Hjertager, B. H., On mathematical modelling of turbulent combustion with special emphasis on soot formation and combustion. In *Sixteenth Symposium (International) on Combustion*. The Combustion Institute, Pittsburgh, PA, 1976, pp. 719–29.
27. Peters, N., Laminar flamelet concepts in turbulent combustion. In *Twenty-first Symposium (International) on Combustion*. The Combustion Institute, Pittsburgh, PA, 1986, pp. 1231–50.
28. Syed, K. J., Stewart, C. D. & Moss, J. B., Modelling soot formation and thermal radiation in buoyant turbulent diffusion flames. In *Twenty-third*

Symposium (International) on Combustion. The Combustion Institute, Pittsburgh, PA, 1990, pp. 1533–41.
29. Babrauskas, V., Burning rates. In *The SFPE Handbook of Fire Protection Engineering*. National Fire Protection Association, Quincy, MA, 1988, pp. 2.1–2.15.
30. Schfiliti, R. P., Design of detection systems. In *The SFPE Handbook of Fire Protection Engineering*. National Fire Protection Association, Quincy, MA, 1988, pp. 3.1–3.21.
31. Briggs, G. A., Plume rise predictions. In *Lectures on Air Pollution and Environmental Impact Analysis*. American Meteorological Society, 1975, pp. 59–111.
32. Pasquill, F. & Smith, F. B., *Atmospheric Diffusion*. Ellis Horwood, Chichester, 1983.
33. Cox, G., Kumar, S., Cumber, P. & Thomson, V., Fire simulation in the design evaluation process: an exemplification of the use of a computer field model. In *Proceedings of the 5th International Interflam Conference*. Interscience, London, 1990, pp. 55–66.
34. Christolis, M. N., Christidou, C. A., Boudouvis, A. G. & Markatos, N. C., Modelling pollutants dispersion around buildings on fire. Paper presented at the International Congress on Air Pollution 95, Porto Carras, Greece, September 1995.